DOI: https://doi.org/10.62985/j.huit_ojs.vol26.no2E.390

ENHANCING SUNFLOWER INSPIRED SOLAR TRACKERS USING ADAPTIVE SIGNAL FILTERING TECHNIQUES

Thanh-Tung Nguyen[1], Son-Truong Ho[1], Thanh-Tuan Nguyen*[1], Xuan-Huy Nguyen[1], Mong-Fong Horng[2], Chin-Shiuh Shieh[2], Thanh-Lam Nguyen[2]

[1]*Faculty of Electrical and Electronics, Nha Trang University, Vietnam*

[2]*Department of Electronic Engineering,*

National Kaohsiung University of Science and Technology, Kaohsiung 807618, Taiwan

*Email: *tuantn@ntu.edu.com*

Received: 12 October 2025; Revised: 18 March 2026; Accepted: 16 April 2026

ABSTRACT

Biologically inspired solar trackers that mimic sunflower motion can improve irradiance capture relative to fixed photovoltaic panels, but sensor noise can destabilize low cost light seeking controllers. This paper presents a sunflower inspired dual axis tracker in which four light dependent resistors (LDRs) are combined with a Kalman filter based preprocessing stage before servo actuation. The contribution lies in the integration of a bio inspired folding mechanism with signal conditioning aimed at reducing spurious control updates, rather than in proposing a new filtering algorithm. Prototype tests show that the tracker produces higher charging power than a fixed south facing panel during a 09:00 to 15:00 measurement window, and the filtered signal yields a smoother control reference under transient cloud disturbances. These findings support the feasibility of the design and indicate that adaptive filtering can improve control stability, although long term durability, actuator energy consumption, and full controller comparison remain for future work.

Keywords: Dual axis solar tracker, Kalman filter, Adaptive signal processing, Energy harvesting efficiency.

1. INTRODUCTION

The global demand for energy is escalating rapidly, driven by industrialization and population growth, necessitating an urgent transition towards sustainable energy sources [1]. Among renewable options, solar photovoltaic (PV) energy is considered one of the most promising solutions due to its abundance and environmental friendliness. To maximize the efficiency of PV systems, it is crucial to maintain the solar panels perpendicular to the incident sun rays throughout the day. Solar tracking systems (STS) have been developed to address this requirement, capable of increasing energy generation significantly compared to fixed tilt installations [2], [3]. Biologically inspired engineering has introduced solar trackers that mimic the heliotropic movement of sunflowers, not only tracking the position of the sun but also folding the panels at night or during adverse weather to protect the mechanical structure [4], [5]. These systems typically rely on photosensors, such as Light Dependent Resistors (LDRs), to detect the direction of maximum light intensity. However, a major challenge facing low cost sensor based trackers is their susceptibility to environmental noise [6]. Factors such as passing clouds, partial shading, or scattered light can cause significant fluctuations in sensor readings. In conventional control systems using simple threshold comparisons, these fluctuations often lead to hunting or mechanical jitter where the motors oscillate continuously

trying to find the optimal position [7]. This instability not only consumes excessive power but also accelerates mechanical wear and reduces the lifespan of the actuators.

To address these limitations, this paper investigates a sunflower inspired dual axis solar tracker that incorporates adaptive signal preprocessing before actuation. The contribution of this study is not the introduction of a new filtering algorithm, because Kalman filtering is already well established. Rather, the novelty lies in the way a bio inspired mechanical structure, a quadrant LDR sensing module, and a lightweight filtering and hysteresis workflow are integrated into a compact proof of concept prototype. Specifically, the paper contributes: (1) a dual axis solar tracking mechanism with a protective folding function inspired by sunflower behavior; (2) an implementation oriented control workflow in which each LDR channel is filtered before the servo commands are updated; and (3) a proof of concept experimental study showing smoother sensing behavior under transient disturbances and higher daytime power output than a fixed panel baseline, while also clarifying the present limits of long term durability and controller comparison. The remainder of this paper is organized as follows: Section 2 describes the hardware design and system implementation. Section 3 details the control algorithm and the Kalman filter design. Section 4 presents the experimental results and discussion, followed by the conclusion in Section 5.

2. SYSTEM HARDWARE DESIGN

The proposed solar tracker features a dual axis mechanism inspired by the heliotropic behavior of sunflowers, allowing the photovoltaic panel to follow the solar trajectory along both the azimuth and elevation directions. The movement of the main axes is driven by MG996R servo motors, which were selected for their high torque capacity and durable metal gear construction, ensuring precise angular adjustments even under wind load. Furthermore, a DC geared motor is utilized to simulate the petal movement, enabling the system to deploy the panels during the day and retract them at night to minimize dust accumulation. The detailed technical specifications of these key components are summarized in Table 1.

Table 1. Technical specifications of the hardware components

Component	Key Specifications	Function
Microcontroller	ATmega328P	Central processing and control
Servo Motor	MG996R	Dual axis tracking actuation
DC Geared Motor	12V, 235 rpm	Panel folding mechanism
Light Sensor	LDR	Solar position detection
Driver Module	L298N	DC motor direction control
Power Supply	Lithium Battery 12V	System energy storage

The integration of these actuators into the frame allows for a robust and flexible mechanical structure. To guarantee operational safety and prevent mechanical overtravel during the folding process, limit switches are strategically installed to provide feedback signals that halt the motor immediately when the panels reach their fully open or closed positions. The central processing unit of the system is the Arduino Uno R3 board, powered by the ATmega328P microcontroller, which is responsible for acquiring sensor data and executing the control algorithms. The sensing module consists of four Light Dependent Resistors (LDRs) separated by opaque baffles. To detect the position of the sun effectively, these sensors are arranged in a quadrant configuration as depicted in Figure 1.

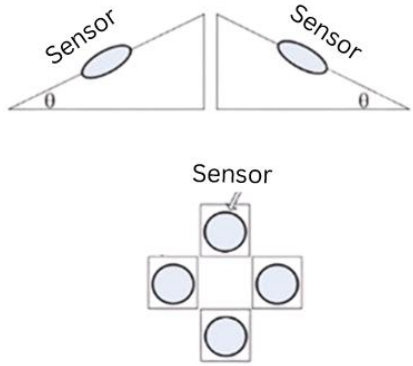

Fig. 1. Physical arrangement and orientation of the sensor module

As illustrated in Figure 2, the four sensors are mounted around a central baffle and oriented toward the east, west, south, and north directions. When the panel is not perpendicular to the sun, the baffle produces an irradiance imbalance across the opposite sensor pairs. This arrangement converts the relative sun position into differential voltage signals that can be used for dual axis tracking.

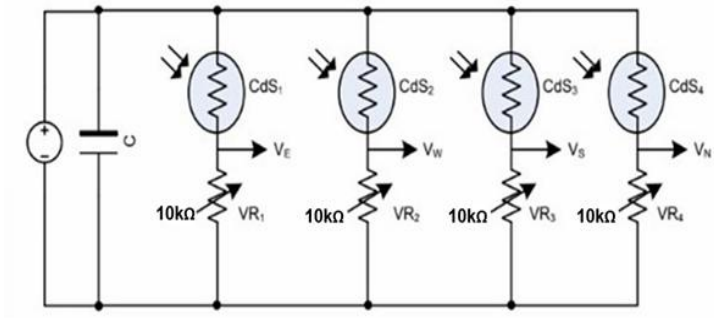

Fig. 2. Circuit diagram of the sensing module using voltage dividers

Each light dependent resistor (LDR) is connected in a voltage divider channel with an adjustable resistor so that the sensing sensitivity can be calibrated during setup. The controller reads four analog voltages corresponding to the east, west, south, and north quadrants, then forms the azimuth and elevation errors from the voltage differences of the opposite pairs. These error signals are subsequently processed by the filtering stage before the servo commands are updated.

3. CONTROL ALGORITHM AND SIGNAL PROCESSING

To ensure precise solar tracking and eliminate the mechanical jitter caused by environmental disturbances, the control system employs a two-stage processing strategy where analog signals are first modeled to represent alignment errors and then processed through a recursive Kalman filter before actuation.

3.1. Formulation of Tracking Error

As established in the hardware design, the sensing unit utilizes four voltage dividers to detect light intensity. The output voltage read by the microcontroller's Analog to Digital Converter (ADC) is mathematically expressed as:

$$V_{out} = V_{CC} \times \frac{R_{fixed}}{R_{LDR} + R_{fixed}} \tag{1}$$

where V_{CC} represents the supply voltage, R_{fixed} denotes the resistance of the fixed resistor, and R_{LDR} is the variable resistance of the photoresistor which decreases with illumination. To determine the solar position, the system calculates the differential potential between opposite sensor pairs for both the azimuth (ΔV_{az}) and elevation (ΔV_{el}) axes using the following equations:

$$\Delta V_{az} = V_E - V_W \tag{2}$$

$$\Delta V_{el} = V_S - V_N \tag{3}$$

where V_E, V_W, V_S, and V_N correspond to the voltage readings from the East, West, South, and North sensors respectively. In an ideal environment, these differential values would be zero when the panel is perpendicular to the sun; however, due to transient noise and environmental scattering, raw values are often unstable and require filtering.

3.2. Adaptive Signal Filtering Design

To mitigate the noise inherent in the sensor readings, a discrete-time Kalman filter is implemented for each channel, operating on the assumption that the true light intensity varies smoothly while measurement noise follows a Gaussian distribution [10]. The state space model of the system at time step k is defined by the linear stochastic difference equations:

$$x_k = x_{k-1} + w_k \tag{4}$$

$$z_k = x_k + v_k \tag{5}$$

where x_k is the true light intensity, z_k is the actual measurement from the ADC, w_k represents the process noise with covariance Q, and v_k represents the measurement noise with covariance R. The recursive estimation process begins with the time update phase, where the algorithm projects the current state and error covariance estimates forward:

$$\hat{x}_k^- = \hat{x}_{k-1} \tag{6}$$

$$P_k^- = P_{k-1} + Q \tag{7}$$

Subsequently, the measurement update phase corrects the predicted estimate using the actual incoming data. The Kalman Gain (K_k), the updated state estimate ($\hat{x}_k$), and the updated error covariance (P_k) are computed as follows:

$$K_k = \frac{P_k^-}{P_k^- + R} \tag{8}$$

$$\hat{x}_k = \hat{x}_k^- + K_k(z_k - \hat{x}_k^-) \tag{9}$$

$$P_k = (1 - K_k)P_k^- \tag{10}$$

By dynamically adjusting the Kalman Gain based on the noise covariance matrices Q and R, the system effectively smooths out high frequency fluctuations caused by passing clouds or electrical noise while maintaining responsiveness to the actual movement of the sun.

In the implemented controller, the same scalar Kalman filter structure is applied to each LDR channel. The state transition and observation coefficients are both set to unity because consecutive light intensity samples are assumed to vary gradually over the sampling interval. The process of noise covariance and measurement noise covariance were tuned empirically during preliminary outdoor trials to balance noise suppression against tracking responsiveness, and the same setting was retained throughout the reported experiments to keep the controller behavior consistent.

After filtering, the controller applies a dead band threshold to the east-west and south-north error signals. Only when the absolute filtered error exceeds this threshold is the corresponding servo angle incremented or decremented; otherwise, the previous angle is maintained to avoid repeated reversals near the alignment point. Because the LDR channels are manually balanced through adjustable resistors, the exact dead band is hardware dependent; therefore, this study reports the tuning logic and control sequence rather than claiming a universally optimal threshold value. The complete acquisition, filtering, and actuation procedure is summarized in Algorithm 1.

Algorithm 1 Adaptive Solar Tracking Control with Kalman Filter

Initialize: $Servo_{az}$, $Servo_{el}$, Threshold ϵ, Q, R, P_0, $\hat{x}_0$
loop
  Read Sensors: z_E, z_W, z_N, z_S from ADC
  for each channel $i \in \{E, W, N, S\}$ **do**
    Predict:
    $P_k^- \leftarrow P_{k-1} + Q$
    Update:
    $K_k \leftarrow P_k^- / (P_k^- + R)$
    $\hat{x}_i \leftarrow \hat{x}_{i(prev)} + K_k \cdot (z_i - \hat{x}_{i(prev)})$
    $P_k \leftarrow (1 - K_k) \cdot P_k^-$
  end for
  Calculate Errors:
  $\Delta V_{az} \leftarrow \hat{x}_E - \hat{x}_W$
  $\Delta V_{el} \leftarrow \hat{x}_S - \hat{x}_N$
  Azimuth Control:
  if $|\Delta V_{az}| > \epsilon$ **then**
    if $\Delta V_{az} > 0$ **then**
      $Servo_{az} \leftarrow Servo_{az} + 1^\circ$
    else
      $Servo_{az} \leftarrow Servo_{az} - 1^\circ$
    end if
  end if
  Elevation Control:
  if $|\Delta V_{el}| > \epsilon$ **then**
    if $\Delta V_{el} > 0$ **then**
      $Servo_{el} \leftarrow Servo_{el} + 1^\circ$
    else
      $Servo_{el} \leftarrow Servo_{el} - 1^\circ$
    end if
  end if
  Wait t_{delay}
end loop

Fig. 3. Algorithm of Adaptive Solar Tracking Control with Kalman Filter

4. EXPERIMENTAL RESULTS AND DISCUSSION

The prototype was evaluated as a proof of concept outdoor study intended to verify three points: the feasibility of the sunflower inspired mechanical structure, the short window energy benefit of active tracking, and the stabilizing role of signal filtering under transient disturbances. The power output comparison reported in Table 2 corresponds to a daytime measurement window from 09:00 to 15:00, while the disturbance case in Figure 5 reflects short cloud related irradiance changes superimposed on sensor noise. Because this initial campaign was not designed as a season long environmental test, the present results should be interpreted as short-horizon validation rather than as a comprehensive durability assessment under all weather conditions. Figure 4 shows the fabricated prototype integrating the LDR sensing module, the servo actuators, and the control unit.

Fig. 4. The fabricated prototype of the sunflower inspired dual axis solar tracker

To evaluate the signal conditioning role of the adaptive filtering stage, the prototype was exposed to transient disturbances such as passing clouds together with ordinary sensor noise. Figure 5 should therefore be read as a signal level comparison between the raw LDR measurements and the filtered reference used by the controller, rather than as a full benchmark between two separately instrumented controllers. The raw trace exhibits rapid fluctuations and a temporary irradiance drop, whereas the filtered trace attenuates these short term disturbances and provides a smoother control reference. This behavior supports the claim that the Kalman stage can reduce unnecessary control reactions; however, the present study does not directly quantify actuator power consumption or long term mechanical wear, so those effects are discussed cautiously.

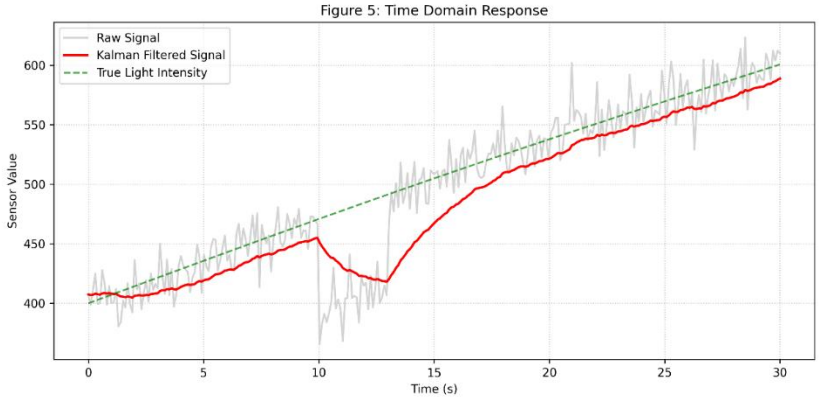

Fig. 5. Time domain response of the sensor signal showing raw versus filtered data

The system level performance metric considered in this study is the charging power gain obtained by active solar tracking relative to a static installation. Field tests were conducted from 09:00 to 15:00 to measure the battery charging power for both the dual axis tracking system and a fixed panel oriented toward the south. This comparison evaluates the overall energy benefit of the prototype with respect to a fixed panel baseline; it should not be interpreted as a complete controller comparison against an unfiltered LDR tracker. For that reason, the controller side benefit of filtering is discussed mainly through the signal behavior in Figure 5, while Table 2 focuses on the net power outcome of the deployed prototype.

Table 2. Power output comparison between the fixed panel and the sunflower inspired dual axis tracker

Time of Day	Power Output - Fixed Panel (W)	Power Output - Dual Axis Tracker (W)	Improvement (%)
09:00	1.23	02.07	68.29
10:00	1.82	2.14	17.58
11:00	02.07	2.19	5.79
12:00	2.42	2.65	9.50
13:00	02.01	2.27	12.93
14:00	1.70	2.19	28.82
15:00	1.61	1.96	21.74

The data in Table 2 show that the dual axis prototype delivers higher charging power than the fixed panel baseline throughout the evaluated time window. The gain is most pronounced in the early morning and late afternoon, when the incidence angle penalizes the stationary panel more severely, while the difference narrows around solar noon as expected. These results support the practical value of active tracking for short window energy capture in the present prototype. At the same time, they do not by themselves establish reduced actuator power consumption, complete oscillation elimination under all disturbances, or long term lifetime extension. A same hardware comparison against a basic unfiltered LDR controller is therefore left as a focused future extension.

5. CONCLUSION

This study presented a sunflower inspired dual axis solar tracker that combines a protective folding mechanism with a Kalman filter assisted sensing and actuation workflow. Within the reported proof of concept tests, the prototype operated stably and produced higher charging power than a fixed south facing panel during the 09:00 to 15:00 evaluation window, with the strongest gains occurring away from solar noon. The signal level results also show that the filtered reference is smoother than the raw LDR measurements under transient disturbances, which supports the use of adaptive filtering to moderate spurious control reactions. However, the contribution of this work lies in the practical integration and validation of these components in a low cost prototype, not in the proposal of a new filtering algorithm.

The present study also has clear limitations. The reported evaluation window is short and does not support broad claims about seasonal robustness, actuator lifetime, or performance under instrumented wind and rainfall conditions. Likewise, the manuscript does not yet include a full controller comparison against an unfiltered LDR tracker using the same hardware platform. These points are therefore treated as future work directions rather than as completed evidence in the current revision.

Acknowledgment: This research is partly funded by Nha Trang University (NTU), Vietnam under grant number ”SV2024-13-61”.

REFERENCES

[1] IEA, *World Energy Outlook 2024*. Paris: IEA, 2024. [Online]. Available: https://www.iea.org/reports/world-energy-outlook-2024

[2] R. Sadeghi, M. Parenti, S. Memme, M. Fossa, and S. Morchio, “A Review and Comparative Analysis of Solar Tracking Systems,” *Energies*, vol. 18, no. 10, Art. no. 2553, May 2025, doi: https://doi.org/10.3390/en18102553.

[3] F. Alam, A. Islam, S. K. Sarker, F. Islam, T. Ahmed, and T. H. Chowdhury, “Design and performance evaluation of dual-axis solar tracking for enhanced photovoltaic efficiency,” *Computer Science and Engineering Research*, vol. 2, no. 1, pp. 41–46, Oct. 2025, doi: https://doi.org/10.69517/cser.2025.02.01.0006.

[4] S. Seme, B. Štumberger, M. Hadžiselimović, and K. Sredenšek, “Solar Photovoltaic Tracking Systems for Electricity Generation: A Review,” *Energies*, vol. 13, no. 16, Art. no. 4224, Aug. 2020, doi: https://doi.org/10.3390/en13164224.

[5] S. Wang *et al*., “Sunflower-like self-sustainable plant-wearable sensing probe,” *Science Advances*, vol. 10, no. 49, Art. no. eads1136, Dec. 2024, doi: https://doi.org/10.1126/sciadv.ads1136.

[6] Z. Li, C. Liu, G. Song, D. Han, Y. Li, and D. Du, “Photovoltaic power generation enhancement performance with a LDR-based dual-axis solar tracking system,” *Clean Technologies and Recycling*, vol. 5, no. 2, pp. 127–142, Sep. 2025, doi: https://doi.org/10.3934/ctr.2025007.

[7] M. Efendi, R. I. Mainil, and A. Aziz, “Comparison of the Efficiency of Solar PV Fixed, Single-Axis, and Dual-Axis Solar Trackers: A Review,” *Jurnal Konversi Energi dan Manufaktur*, vol. 10, no. 1, pp. 84–93, Jan. 2025, doi: https://doi.org/10.21009/JKEM.10.1.9.

[8] M. Al-Sheikh, “IoT-Enabled Dual-Axis Solar Tracking System Using ESP32 and Blynk for Real-Time Monitoring and Energy Optimization,” *Jupiter: Publikasi Ilmu Keteknikan Industri, Teknik Elektro dan Informatika*, vol. 3, no. 1, pp. 187–204, Jan. 2025, doi: https://doi.org/10.61132/jupiter.v3i1.695.

[9] J. S. Valdez-Martínez *et al*., “Kalman Filter-Based Reconstruction of Power Trajectories for IoT-Based Photovoltaic System Monitoring,” *Mathematics*, vol. 14, no. 1, Art. no. 144, 2026, doi: https://doi.org/10.3390/math14010144.

[10] A. Pirayawaraporn, S. Sappaniran, S. Nooraksa, C. Prommai, N. Chindakham, and C. Jamroen, “Innovative sensorless dual-axis solar tracking system using particle filter,” *Applied Energy*, vol. 338, Art. no. 120946, May 2023, doi: https://doi.org/10.1016/j.apenergy.2023.120946.